WAVE PROPAGATION IN A MAGNETICALLY STRUCTURED ATMOSPHERE

III: *The Slab in a Magnetic Environment*

P. M. EDWIN and B. ROBERTS

Department of Applied Mathematics, University of St. Andrews, St. Andrews, Fife, Scotland

(Received 27 January; in revised form 5 June, 1981)

Abstract. The propagation of waves in a magnetic slab embedded in a magnetic environment is investigated. The possible modes of propagation are examined from the *general* dispersion relation, both analytically and numerically, for disturbances which are evanescent in the environment. Approximate dispersion relations governing propagation in a *slender* slab of field are derived both from the general dispersion relation and from an application of the slender flux tube approximation.

Several different situations, representative of both photospheric and coronal conditions, are considered. In general, the structures are found to support both fast and slow, *body* and *surface*, waves. Under coronal conditions, for two dimensional propagation, disturbances propagate as fast and slow body waves. The fast body waves are analogous to the ducted shear waves of seismology (Love waves).

1. Introduction

The magnetically structured nature of the solar atmosphere, as made manifest in EUV- and X-ray lines, suggests that the usual picture of the propagation of magnetohydrodynamic waves in a uniform medium is inapplicable in the solar context. In particular, a sharply structured atmosphere can support magneto-acoustic *surface waves*, which may be classified as either fast or slow modes. Additionally, a new characteristic speed of propagation becomes important.

In a uniform medium, magnetohydrodynamic waves are generally discussed in terms of the sound speed c_0, Alfvén speed v_A and (perhaps) fast speed $(c_0^2 + v_A^2)^{1/2}$. However, there is another speed, c_T, defined by

$$c_T = c_0 v_A / (c_0^2 + v_A^2)^{1/2},$$

which is present in the uniform medium but whose importance has generally been overlooked. It is both sub-sonic and sub-Alfvénic; in the corona, for example, c_T is slightly below the local sound speed. In a sharply structured medium, though, the importance of c_T is readily apparent. In an isolated flux tube, for example, c_T is the upper bound on the phase-speed of the slow magnetoacoustic wave (Roberts, 1981b), the bound being attained for modes of long wavelength (Defouw, 1976; Roberts and Webb, 1978).

In Roberts (1981a, b; Papers I and II) we reviewed the equations for wave propagation in a structured medium, and investigated those equations for the particular cases of a single interface and an isolated magnetic slab (see also Wentzel, 1979a, b). Our main concern was to illuminate the properties of surface waves. To do this it was convenient to pay particular attention to the circumstances of one

Solar Physics **76** (1982) 239–259. 0038–0938/82/0762–0239 $03.15.

region of the structured atmosphere being field-free. Such a choice in field distribution is of obvious relevance to photospheric conditions, where isolated flux tubes represent over 90% of the observed flux distribution, but coronal conditions are clearly different. Indeed, in the corona structuring arises principally through spatial variations in density and temperature; field variations are likely to be slight. Nonetheless, marked spatial variations in Alfvén and sound speeds are expected and so the possibility of surface waves arises.

We turn here, then, to an examination of the influence of structuring on wave propagation in a medium permeated by magnetic field. Our study extends the analysis in Roberts (1981b) to include the effect of a magnetic field external to a slab. Such an investigation allows us to shed additional light on the basic physics of magnetoacoustic wave propagation in an inhomogeneous atmosphere; furthermore, it enables us to examine which modes are likely to arise in the solar corona. In such a low-β plasma, it transpires, two-dimensional disturbances propagate as body waves (with oscillatory structure inside the slab of field and evanescent structure outside the slab), which may be either fast (Alfvénic phase-speeds) or slow (acoustic phase-speeds). The fast magnetoacoustic body waves of the corona are mathematically analogous to the ducted shear waves of seismology first explored by Love (1911).

2. The Dispersion Relation

Our starting point is the equilibrium state of an ideal gas permeated by a non-uniform magnetic field $B_0(x)\hat{\mathbf{z}}$, where x, y, z denote the usual Cartesian coordinates. The density $\rho_0(x)$ and temperature $T_0(x)$ are structured, as is the pressure $p_0(x)$. But equilibrium demands that the total (gas plus magnetic) pressure is uniform:

$$\frac{\mathrm{d}}{\mathrm{d}x}\left(p_0+\frac{B_0^2}{2\mu}\right)=0\,. \tag{1}$$

Linear perturbations about the above equilibrium state may be described by the equations of continuity, momentum, induction, and isentropic energy. The effect of gravity will be ignored. Considering two-dimensional velocity disturbances $\mathbf{v}$ of the form

$$\mathbf{v}=(v_x,\,0,\,v_z)\,,\qquad v_x=\hat{v}_x(x)\,e^{i\omega t+ikz}\,,\qquad v_z=\hat{v}_z(x)\,e^{i\omega t+ikz}\,, \tag{2}$$

where k is the longitudinal wavenumber and ω is the frequency, we may show (see Paper I; Goedbloed, 1971) that the amplitude $\hat{v}_x(x)$ of the disturbance normal to the applied field satisfies the equation

$$\frac{\mathrm{d}}{\mathrm{d}x}\left\{\frac{\rho_0(x)(c_0^2(x)+v_\mathrm{A}^2(x))(k^2c_T^2(x)-\omega^2)}{(k^2c_0^2(x)-\omega^2)}\frac{\mathrm{d}\hat{v}_x}{\mathrm{d}x}\right\}-$$

$$-\rho_0(x)(k^2v_\mathrm{A}^2(x)-\omega^2)\hat{v}_x=0\,, \tag{3}$$

where

$$c_0=\left(\frac{\gamma p_0}{\rho_0}\right)^{1/2}, \qquad v_A=\frac{B_0}{(\mu\rho_0)^{1/2}}, \qquad c_T=\frac{c_0 v_A}{(c_0^2+v_A^2)^{1/2}}.$$

Here γ is the ratio of specific heats and μ the magnetic permeability.

For future reference, we may note that the component of velocity along the field, $\hat{v}_z(x)$, and the total pressure perturbation $\hat{p}_T$ are related to $\hat{v}_x(x)$ by (see Paper I, Equations (17) and (18))

$$\hat{v}_z(x)=\frac{ikc_0^2}{(k^2c_0^2-\omega^2)}\frac{d\hat{v}_x}{dx}, \qquad \hat{p}_T(x)=\frac{i\rho_0}{\omega}(c_0^2+v_A^2)\frac{(k^2c_T^2-\omega^2)}{(k^2c_0^2-\omega^2)}\frac{d\hat{v}_x}{dx}. \tag{4}$$

In a *uniform* medium, the coefficients of (3) are all constants and so it may be written in the form

$$\frac{d^2\hat{v}_x}{dx^2}-m_0^2\hat{v}_x=0, \tag{5}$$

where

$$m_0^2=\frac{(k^2c_0^2-\omega^2)(k^2v_A^2-\omega^2)}{(c_0^2+v_A^2)(k^2c_T^2-\omega^2)}.$$

If the uniform medium is also *unbounded*, then a normal mode of the form $\hat{v}_x(x)\sim e^{inx}$, for wavenumber n transverse to the field, is permissible, with ω satisfying the equation

$$n^2+m_0^2=0. \tag{6}$$

Written out in full, (6) is immediately recognisable as the usual dispersion relation (in two-dimensional form) for fast and slow magnetoacoustic waves.

Returning to (5), we consider now an example of a structured medium. We suppose that the equilibrium consists of a slab of uniform field $B_0\hat{\mathbf{z}}$ confined to a region $|x|<x_0$, outside of which the field is $B_e\hat{\mathbf{z}}$, the gas pressure p_e, and the density ρ_e (see Figure 1). Thus, the equilibrium state may be described by

$$p_0(x),\rho_0(x),B_0(x)=\begin{cases}p_0,\rho_0,B_0, & |x|<x_0,\\ p_e,\rho_e,B_e, & |x|>x_0.\end{cases} \tag{7}$$

Equation (1) shows that

$$p_0+\frac{B_0^2}{2\mu}=p_e+\frac{B_e^2}{2\mu}, \tag{8}$$

which may be combined with the ideal gas law to give

$$\frac{\rho_e}{\rho_0}=\frac{c_0^2+\frac{1}{2}\gamma v_A^2}{c_e^2+\frac{1}{2}\gamma v_{Ae}^2}, \tag{9}$$

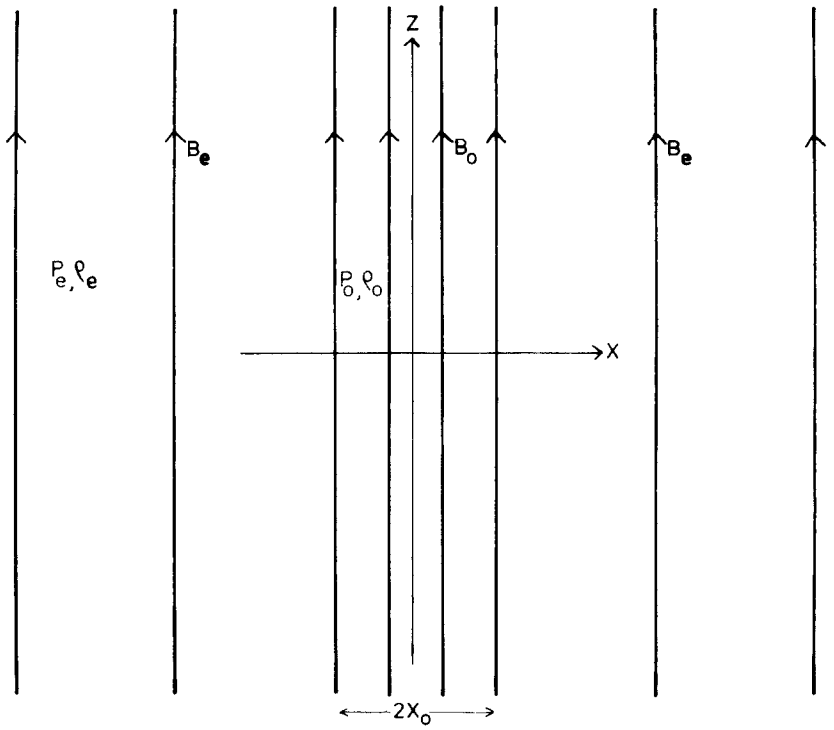

Fig. 1. The equilibrium structured atmosphere.

where $c_e = (\gamma p_e/\rho_e)^{1/2}$ and $v_{Ae} = B_e/(\mu\rho_e)^{1/2}$ are the sound and Alfvén speeds in the 'external' ($|x| > x_0$) medium.

Since both $|x| > x_0$ and $|x| < x_0$ are uniform media, perturbations about the equilibrium (7)–(9) may be described by Equation (5). We will confine our attention to disturbances that are laterally *evanescent* in $|x| > x_0$, so that $\hat{v}_x \to 0$ as $|x| \to \infty$ and the energy of the disturbance is essentially confined to the interior of the slab. Equation (5) then gives

$$\hat{v}_x(x) = \begin{cases} \alpha_e e^{-m_e(x-x_0)}, & x > x_0, \\ \alpha_0 \cosh m_0 x + \beta_0 \sinh m_0 x, & |x| < x_0, \\ \beta_e e^{m_e(x+x_0)}, & x < -x_0, \end{cases} \tag{10}$$

where α_0, β_0, α_e, β_e are arbitrary constants, and m_e is given by

$$m_e^2 = \frac{(k^2 c_e^2 - \omega^2)(k^2 v_{Ae}^2 - \omega^2)}{(c_e^2 + v_{Ae}^2)(k^2 c_{Te}^2 - \omega^2)}, \qquad c_{Te}^2 = \frac{c_e^2 v_{Ae}^2}{(c_e^2 + v_{Ae}^2)}.$$

In writing (10) we have supposed that m_e is positive, corresponding to evanescent solutions outside of the slab. However, m_0^2 may be positive or negative. (If the condition $m_e > 0$ is not imposed, then the slab may act as a radiator of waves which

corresponds to m_e (and ω) being complex. Some discussion of these circumstances may be found in Roberts and Webb (1979) and, more fully, in Spruit (1982).)

The constants in (10) are related by requiring that $\hat{v}_x(x)$ and $\hat{p}_T(x)$ be continuous across $x = \pm x_0$. For a non-trivial solution under these conditions we must have

$$\rho_e(k^2 v_{Ae}^2 - \omega^2) m_0 \begin{Bmatrix} \tanh \\ \coth \end{Bmatrix} m_0 x_0 + \rho_0(k^2 v_A^2 - \omega^2) m_e = 0\,, \tag{11}$$

where the tanh/coth terms correspond to the sinh/cosh solutions in (10). Equation (11) is the dispersion relation governing disturbances in a slab of field B_0 embedded in an external field B_e. It applies for $m_e > 0$ only.

3. Surface and Body Waves

We consider now the properties of the dispersion relation. Since (11) is transcendental, we expect it to possess a rich spectrum of solutions. To classify these normal modes, we shall refer to solutions with $m_0^2 > 0$ as *surface* waves, and those with $m_0^2 < 0$ as *body* waves (see Papers I and II for further discussion). Additionally, waves may be classified as *sausage* modes or *kink* modes, accordingly as the 'tanh' or 'coth' functions are used in (11), corresponding to $\hat{v}_x$ being an odd or even function of x.

There are a number of immediate deductions from (11). For example, it is clear that surface waves ($m_0^2 > 0$) can only arise if the longitudinal phase-speed ω/k of a disturbance lies between the two Alfvén speeds, v_A and v_{Ae}. Much the same feature arises at a single magnetic interface (Wentzel, 1979a) and, as for the single interface, the possibility of *two* surface waves arises (Paper I). Finally, we observe that the condition $m_e^2 > 0$ implies that (11) possesses solutions only for

$$\omega < kc_{Te}, \text{ or } \min(kv_{Ae}, kc_e) < \omega < \max(kv_{Ae}, kc_e).$$

In the limit of zero external field ($v_{Ae} = 0$), (11) reduces to (10) of Paper II. In Paper II it was shown that the dispersion relation permits slow magnetoacoustic surface waves which propagate with longitudinal phase-speed below c_T. If, however, there is an external magnetic field present, so that (11) above applies, waves with phase-speeds below c_T arise only if $v_{Ae} < c_T (< v_A)$, for otherwise we would violate the requirement that the phase-speed lie between the two Alfvén speeds. Of course, even the possibility of phase-speeds below c_T is ruled out if both v_{Ae} and c_e are less than c_T (because for $m_e^2 > 0$ there are no solutions for $\omega > \max(kv_{Ae}, kc_e)$). There are thus a number of important modifications to be made to the dispersion diagrams presented in Paper II. To present these new findings it is convenient to treat a number of special cases.

3.1. Incompressible Motions

For an incompressible fluid, corresponding to $\gamma \to \infty$ in (11), both m_0 and m_e tend to k; the modes are thus Alfvén surface waves. The dispersion relation governing

Alfvén surface waves is

$$\frac{\omega^2}{k^2} = \frac{\rho_0 v_A^2 + \rho_e v_{Ae}^2 \left\{ \begin{matrix} \tanh \\ \coth \end{matrix} \right\} kx_0}{\rho_0 + \rho_e \left\{ \begin{matrix} \tanh \\ \coth \end{matrix} \right\} kx_0}. \tag{12}$$

(For the cylindrical equivalent of (12) see Uberoi and Somasundaram (1980).)

For long waves in a slender slab, $kx_0 \ll 1$, (12) reduces to

$$\omega^2 \simeq k^2 v_A^2 \{1 + \rho_e/\rho_0 (v_{Ae}^2/v_A^2 - 1) kx_0\} \tag{13a}$$

for the sausage mode,* and

$$\omega^2 \simeq k^2 v_{Ae}^2 \{1 + \rho_0/\rho_e (v_A^2/v_{Ae}^2 - 1) kx_0\} \tag{13b}$$

for the kink mode. In a wide slab, $kx_0 \gg 1$, both modes have phase-speeds given by

$$\frac{\omega^2}{k^2} \simeq \frac{\rho_e v_{Ae}^2 + \rho_0 v_A^2}{\rho_e + \rho_0}. \tag{14}$$

It is clear from the above that the general behaviour of the phase-speeds of the sausage and kink modes interchanges, accordingly as v_{Ae} is greater or less than v_A. The phase-speed as a function of kx_0 is sketched in Figure 2 for the cases $v_A > v_{Ae}$ and $v_A < v_{Ae}$.

3.2. Compressible Modes

Returning to the general dispersion relation (11), we consider the spectrum of compressible waves. These are more difficult to investigate than the incompressible modes, mainly because of the transcendental nature of (11) with m_0 and m_e functions of ω. One special case of particular interest, that is also amenable to an analytical investigation, is the *slender* slab, corresponding to $kx_0 \ll 1$, i.e., to waves with wavelengths very much greater than the width of the slab. This is of interest for both photospheric and coronal applications. In the photosphere, most of the magnetic flux occurs in isolated, thin flux tubes, the environment of a tube being essentially field-free ($v_{Ae} = 0$). In the corona, the observed loop structure suggests narrow regions of inhomogeneity: photographs of coronal loops indicate structures that are (say) one-tenth as wide as they are long (corresponding to aspect ratios of about 10). We consider the slender slab in Section 3.2.1, treating a slab of finite dimension in Section 3.2.2.

3.2.1. *Slender Slab*

Consider, then, the reduction of (11) in the limit of small kx_0. We suppose that $m_0 x_0 \to 0$ as $kx_0 \to 0$, so that $\tanh m_0 x_0 \simeq m_0 x_0$ for $kx_0 \ll 1$. (The results derived by

* It may be noted in passing that (13a) indicates a *faster* fall-off in phase-speed with increasing kx_0 ($\ll 1$) than occurs in a *cylindrical* flux tube (see Roberts and Webb, 1978).

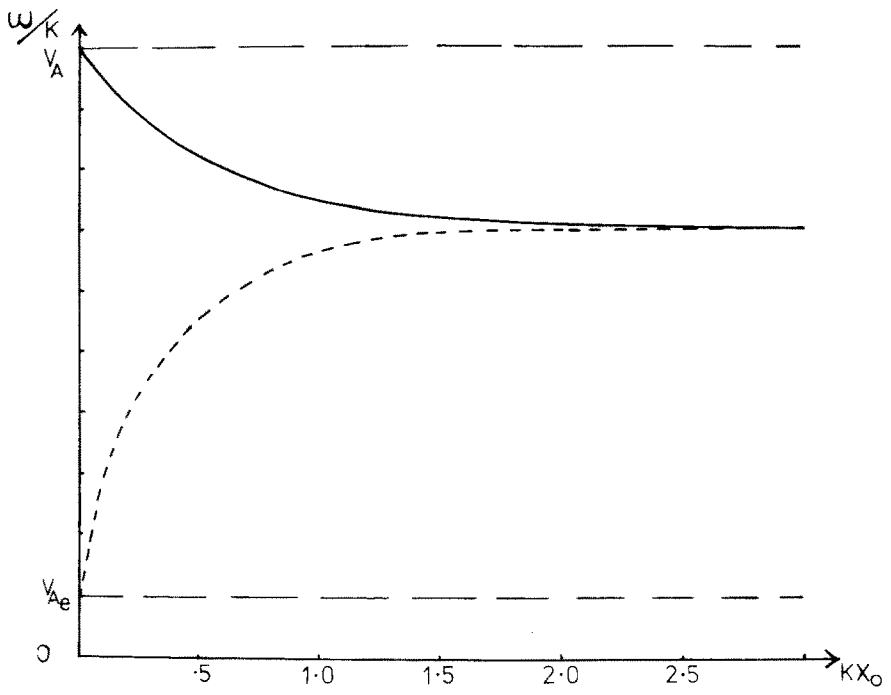

(a)

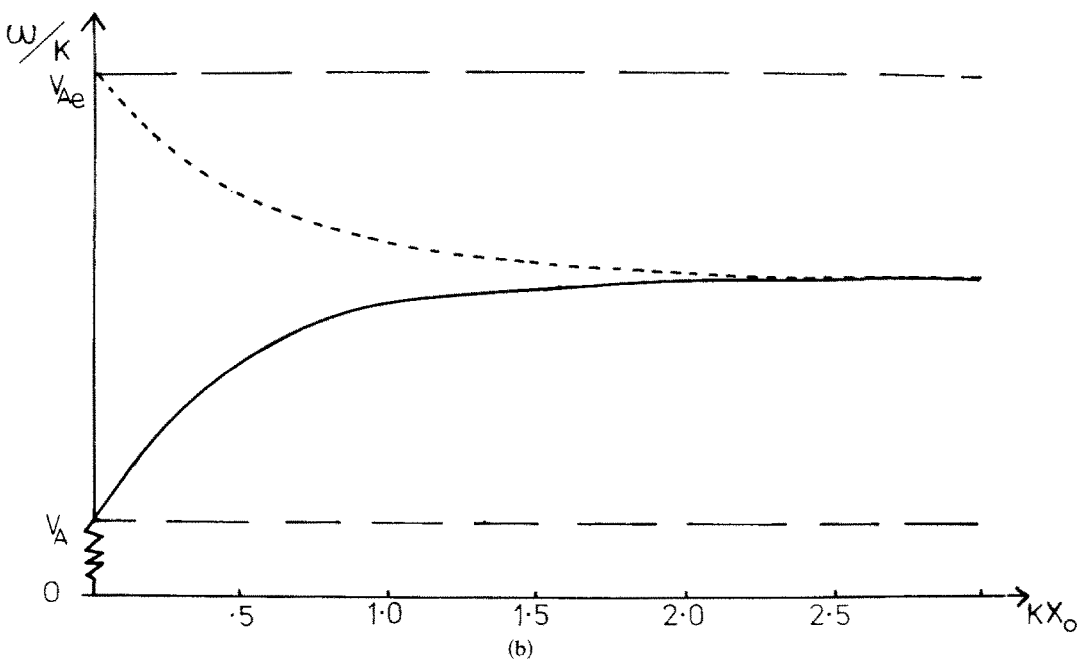

(b)

Fig. 2. The phase-speed ω/k as a function of kx_0 for Alfvén surface waves in an incompressible medium. We have taken $\rho_0 = \rho_e$ and illustrated the case $v_A > v_{Ae}$ (here $v_{Ae} = 0.1\, v_A$) in (a) and $v_A < v_{Ae}$ (here $v_{Ae} = 1.5\, v_A$) in (b). ———: Sausage mode; – – –: Kink mode.

such an analysis must be checked *a posteriori*; see Roberts and Webb (1979) and Wilson (1980).) Under such circumstances, (11) reduces to

$$\rho_0(k^2v_A^2-\omega^2)m_e+\rho_e(k^2v_{Ae}^2-\omega^2)m_0^2x_0=0 \tag{15}$$

for the *sausage* mode ('tanh' function), and this has approximate solutions:

$$\omega^2\simeq k^2c_e^2\left\{1+\left(\frac{\rho_e}{\rho_0}\right)^2\frac{(c_0^2-c_e^2)^2(v_{Ae}^2-c_e^2)c_e^2}{(c_T^2-c_e^2)^2(c_0^2+v_A^2)^2}(kx_0)^2\right\}, \tag{16a}$$

$$\omega^2\simeq k^2c_T^2\left\{1+\left(\frac{\rho_e}{\rho_0}\right)\frac{(c_0^2-c_T^2)(v_{Ae}^2-c_T^2)^{1/2}(c_e^2+v_{Ae}^2)^{1/2}(c_{Te}^2-c_T^2)^{1/2}(kx_0)}{(c_e^2-c_T^2)^{1/2}(c_0^2+v_A^2)c_T^2}\right\},$$

$$c_{Te}>c_T, \tag{16b}$$

$$\omega^2\simeq k^2c_T^2\left\{1+\left(\frac{\rho_e}{\rho_0}\right)\frac{(c_0^2-c_T^2)(v_{Ae}^2-c_T^2)^{1/2}(c_e^2+v_{Ae}^2)^{1/2}(c_T^2-c_{Te}^2)^{1/2}(kx_0)}{(c_T^2-c_e^2)^{1/2}(c_0^2+v_A^2)c_T^2}\right\},$$

$$v_{Ae}>c_T>c_e, \tag{16c}$$

and

$$\omega^2\simeq k^2c_T^2\left\{1-\left(\frac{\rho_e}{\rho_0}\right)\frac{(c_0^2-c_T^2)(c_T^2-v_{Ae}^2)^{1/2}(c_e^2+v_{Ae}^2)^{1/2}(c_T^2-c_{Te}^2)^{1/2}(kx_0)}{(c_e^2-c_T^2)^{1/2}(c_0^2+v_A^2)c_T^2}\right\},$$

$$c_e>c_T>v_{Ae}. \tag{16d}$$

It may be noted that (16a) and (16d) for the special case $v_{Ae}=0$ agree with the results in Paper II.

It is clear from Equations (16) that the sausage modes in a slender slab are only weakly affected by the presence of an external field. The mode described by (16a) corresponds to a fast disturbance, those in (16b, c, d) to a slow disturbance; the external pressure perturbation is negligible for the slow mode but not for the fast mode (Roberts, 1981b; Webb, 1980).

In the limit of $kx_0\ll 1$, the reduction of (11) for the *kink* mode leads to

$$\rho_e(k^2v_{Ae}^2-\omega^2)+\rho_0(k^2v_A^2-\omega^2)m_ex_0=0, \tag{17}$$

which may be solved to give

$$\omega^2\simeq k^2v_{Ae}^2\left\{1-\left(\frac{\rho_0}{\rho_e}\right)^2\left(1-\frac{v_A^2}{v_{Ae}^2}\right)\left(1-\frac{c_e^2}{v_{Ae}^2}\right)(kx_0)^2\right\}, \tag{18a}$$

provided v_{Ae}/v_A is not $O(kx_0)$, and

$$\omega^2\simeq k^2c_{Te}^2\left\{1-\left(\frac{\rho_0}{\rho_e}\right)^2\frac{(c_{Te}^2-v_A^2)^2(c_e^2-c_{Te}^2)(kx_0)^2}{v_{Ae}^4c_{Te}^2}\right\}, \qquad c_{Te}>v_A. \tag{18b}$$

If v_{Ae}/v_A is $O(kx_0)$, and thus $v_{Ae}\ll v_A$ for $kx_0\ll 1$, then Equations (18) do not hold. Instead, solving (17) in this limit gives

$$\omega^2\simeq k^2v_{Ae}^2\left\{1+\frac{\rho_0}{\rho_e}\frac{v_A^2}{v_{Ae}^2}(kx_0)\right\}, \qquad v_{Ae}\to 0. \tag{19}$$

This is the case discussed in Paper II.

Thus, provided the slab is sufficiently narrow its behaviour in the kink mode is dictated by the external, non-zero, magnetic field, the narrow band of field lines being vibrated by the surrounding medium. If the combined effects of external gas and magnetic pressure are sufficiently weak, so that $c_{Te} < v_A$ and (18b) is inapplicable, then only one mode occurs (given either by (18a) or (19)). If the external magnetic field is negligible, only the mode (19) is pertinent.

We should note that equations equivalent to (15)–(18) have also been obtained by Chakraborty (1968) in the context of investigating a two-dimensional compressible jet. However, Chakraborty's analysis was primarily concerned with the stability aspects of the jet rather than the wave structure which is of chief concern here.

It is interesting to observe that the approximate dispersion relations for the sausage and kink modes, namely, (15) and (17) respectively, may be derived directly by adopting the slender flux tube equations in an *ab initio* approach. The details of such an argument, which are similar to those given in Paper II for the slab in a field-free environment, are outlined in the Appendix.

The dispersion relations (15) and (17), for the sausage and kink modes in a slender slab, do not exhaust all the possible modes in a slab. Indeed, a scrutiny of the general dispersion relation, in the special case $v_{Ae} = 0$ (see Roberts and Webb, 1979; Roberts, 1981b), reveals that there are solutions with $m_0 x_0 \not\to 0$ as $kx_0 \to 0$. Such modes correspond to body waves which, in general, oscillate rapidly across the width of the slab. Some analytical results for these modes may be found (as in Paper II), but the results are generally unwieldy. Instead, it is convenient to turn to a computational solution of the dispersion relation; we examine, in general, the structure of waves in a slab of finite width.

3.2.2. *The Finite Slab*

The computer solution of the general dispersion relation (11) is presented in Figures 3–7, chosen to cover a number of illustrative cases that are either of particular relevance to solar applications or illuminate an aspect of the basic physics of slab waves. In general, a slab may support both fast and slow surface waves and fast and slow body waves.

Some indication of which waves are present in each case may be gained from consideration of the general dispersion relation (11) in the limit of large kx_0. For both kink and sausage modes this results in the relation

$$m_0\rho_e(k^2 v_{Ae}^2 - \omega^2) + m_e\rho_0(k^2 v_A^2 - \omega^2) = 0\,, \tag{20}$$

which may be reduced to a cubic and solved to determine which modes are present. Equation (20) is also considered by Wentzel (1979a); it describes the situation pertaining at a single interface between two non-zero magnetic fields.

We consider first, in Figure 3, the effect of a small, non-zero, external magnetic field. The harmonics of slow body waves are present and are confined to the region $c_T < \omega/k < c_0$. There are two surface waves in the sausage mode, as for the case of zero external field, but there are also two in the kink mode. The slow kink mode,

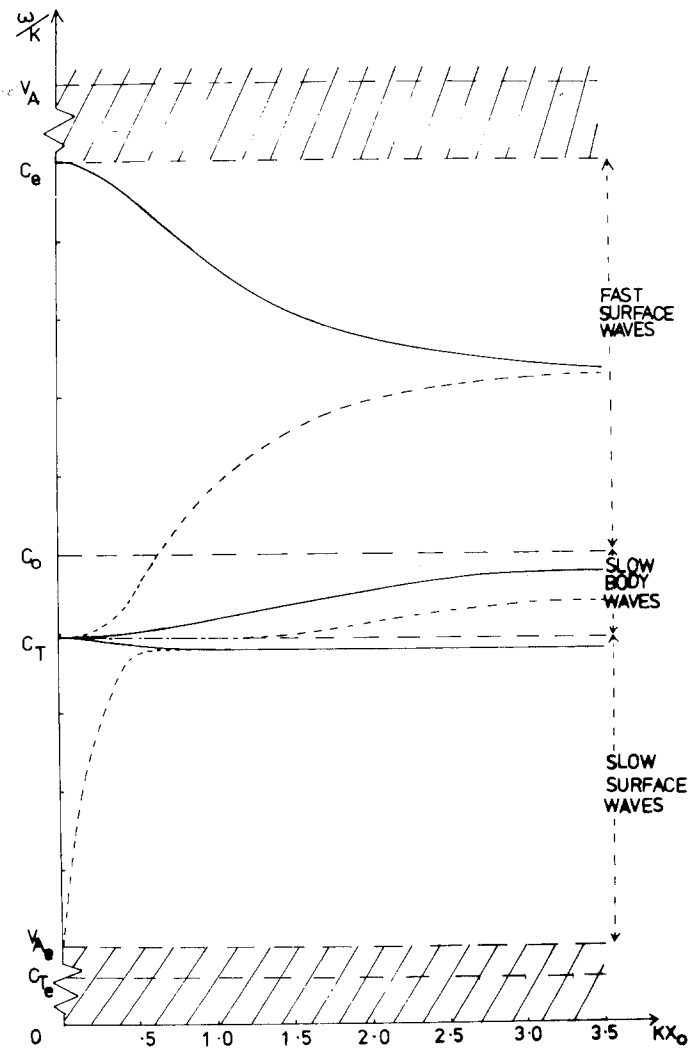

Fig. 3. The phase-speed ω/k as a function of kx_0, showing that, for small exterior magnetic field (here illustrated for $v_{Ae} = 0.5\, c_0$, $c_e = 1.5 c_0$ and $v_A = 2.0 c_0$), two sets of surface waves ($m_0^2 > 0$) exist. There is a band of body waves ($m_0^2 < 0$) for $c_T < \omega/k < c_0$ of which only two typical modes are shown. Hatching indicates regions where waves do not occur. ———: Sausage mode; – – – –: Kink mode.

for a slender slab, is given by Equation (19). The fast kink mode appears to change in character from a body to a surface wave as the phase-speed passes through the slab's sound speed. (The form of the velocity component $\hat{v}_x$ with variation in slab width, for this fast kink wave, was plotted in this transition region and shows that for both body and surface waves near $\omega/k = c_0$ the profile is approximately uniform across the slab. Of course, for $\omega/k = c_0$ the longitudinal velocity is arbitrary along the slab instead of being determined by Equation (4).*)

* Equation (11) possesses degenerate solutions, $\omega^2 = k^2 c_0^2$, $k^2 c_e^2$, $k^2 v_A^2$ and $k^2 v_{Ae}^2$.

Figure 1b (Paper II), which describes the limiting case of $v_{Ae} = 0$, and Figure 3 are similar except that a fast kink surface mode, arising from a body wave, was overlooked in Paper II and should in fact have appeared in Figure 1b of that paper. The slender slab approximation does not predict this fast kink surface wave, which has a phase-speed equal to the sound speed at an *intermediate* value of kx_0. In fact, this value of kx_0 may be deduced from Equation (10) of Paper II (Equation (11) with $v_{Ae} = 0$ here); the surface wave arises at

$$kx_0 \simeq (c_0^2 + \gamma v_A^2/2)c_0^2/(v_A^2 - c_0^2)(c_e^2 - c_0^2)^{1/2} c_e .$$

In Figure 4 we have sketched a case typical of coronal conditions with low plasma β both inside the slab and in its environment. As a result of decreasing β in the

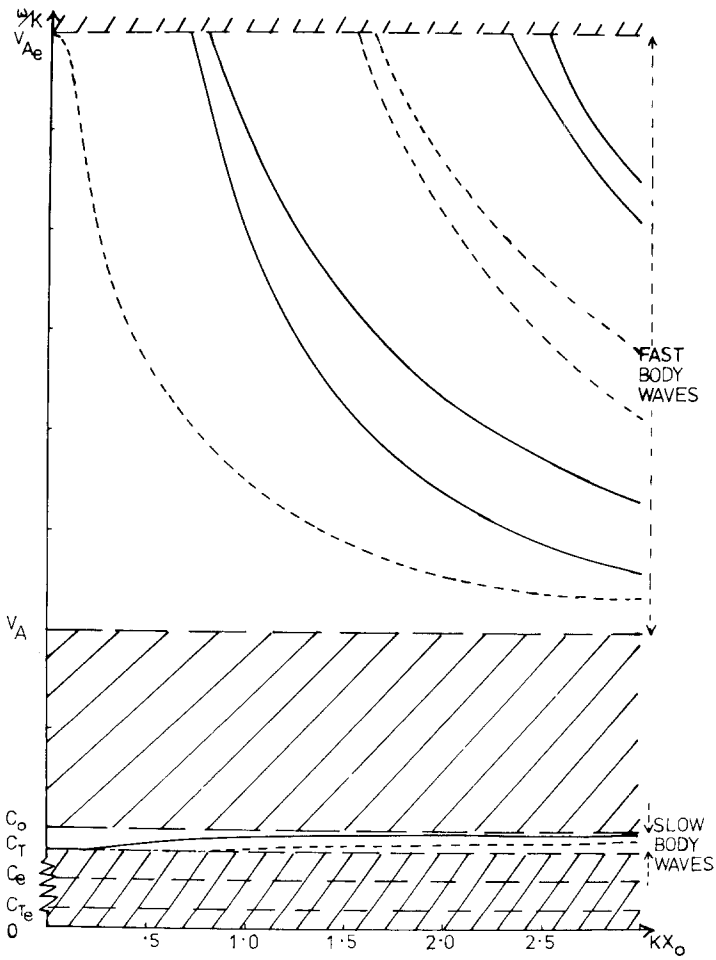

Fig. 4. The phase-speed ω/k as a function of kx_0 under circumstances (here illustrated for $v_{Ae} = 5c_0$, $c_e = 0.5c_0$ and $v_A = 2c_0$) representative of coronal conditions. The results show that only the two sets of body waves ($m_0^2 < 0$) exist. The narrow band of slow waves contains infinitely many harmonics of which only two are shown. Hatching denotes regions in which there are no waves. ———: Sausage mode; - - - -: Kink mode.

slab's exterior we now have a quite different situation to that described in Figure 3. There are now no surface ($m_0^2 > 0$) waves; but harmonics arise in the two regions $c_T < \omega/k < c_0$ and $v_A < \omega/k < v_{Ae}$, corresponding to slow and fast body ($m_0^2 < 0$) waves respectively. The same result holds if the external temperature is the higher one, that is if the sound speeds are interchanged. However, if the internal Alfvén speed is the higher, so that the Alfvén speeds are interchanged, only the slow harmonics remain.

The extreme $c_e = c_0 = 0$, the cold plasma approximation, is of interest. This eliminates the narrow band of slow body waves in the lower part of Figure 4, but the fast waves are described by

$$\rho_e \frac{m_e}{v_A^2} \left\{ \begin{matrix} \tan \\ -\cot \end{matrix} \right\} q_0 x_0 = -\frac{\rho_0 q_0}{v_{Ae}^2}, \tag{21}$$

where

$$q_0^2 = \left(\frac{\omega}{v_A}\right)^2 - k^2, \qquad m_e^2 = k^2 - \left(\frac{\omega}{v_{Ae}}\right)^2.$$

Both q_0^2 and m_e^2 are positive for $v_A < \omega/k < v_{Ae}$. Thus the fast sausage modes are the roots of

$$\tan q_0 x_0 = -q_0/m_e, \tag{22}$$

and the fast kink modes are given by

$$\tan q_0 x_0 = m_e/q_0. \tag{23}$$

It is a curious fact that Equation (23) is precisely Love's equation (Love, 1911; see also Ewing *et al.*, 1957, p. 210). Love's equation, it will be recalled, arises in the propagation of waves in a layered elastic material such as the Earth's crust. Furthermore, an equation analogous to (22) for the sausage mode may also be found in seismic studies (see Ewing *et al.*, p. 138).

The situation $c_e > c_0 > v_A$, $v_{Ae} = 0$ was discussed in Paper II. Since we now have the means to include a non-zero magnetic field exterior to the slab, we consider the effect of the speed v_{Ae} lying in the region between c_0 and v_A – a region which had no modes for the slab in a field-free environment. Thus Figure 5 illustrates the configuration, $c_e > c_0 > v_{Ae} > v_A$. Though there are body waves confined to the region between the two sound speeds there is now no fast surface kink mode (cf. Figure 3). There are no modes in the region between c_{Te} and c_0. The slow sausage surface wave exhibits a similar property to that mentioned earlier, of appearing to change in character from a body to a surface wave as the phase-speed passes through the slab's Alfvén speed.

Again, we may draw an analogy with Love waves by using the approximation $v_A = v_{Ae} = 0$, for it is clear that in such circumstances there are only fast body waves, occupying the region $c_0 < \omega/k < c_e$. Now with $v_A = v_{Ae} = 0$, the general dispersion

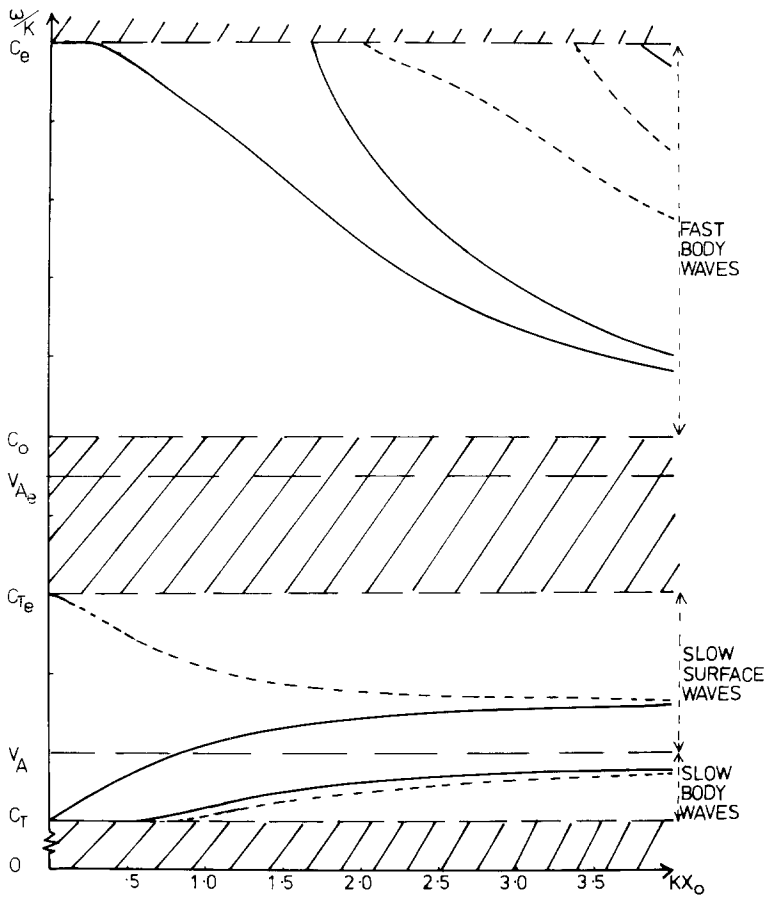

Fig. 5. The phase-speed ω/k as a function of kx_0 (illustrated for $v_{Ae} = 0.95c_0$, $c_e = 1.5c_0$ and $v_A = 0.6c_0$). Only two typical body waves ($m_0^2 < 0$) of the infinite number occurring in $c_T < \omega/k < v_A$ are shown. The hatching denotes regions in which modes do not occur. ———: Sausage mode; - - - -: Kink mode.

relation reduces to (see also Equation (22) in Paper II)

$$\tan n_0 x_0 = \left(\frac{c_e^2}{c_0^2}\right) \frac{m_e}{n_0} \tag{24}$$

for the sausage mode, and

$$\tan n_0 x_0 = -\left(\frac{c_0^2}{c_e^2}\right) \frac{n_0}{m_e} \tag{25}$$

for the kink. In (24) and (25),

$$n_0^2 = \left(\frac{\omega}{c_0}\right)^2 - k^2, \qquad m_e^2 = k^2 - \left(\frac{\omega}{c_e}\right)^2,$$

and both are positive (so $c_0 < \omega/k < c_e$). Equation (24) is equivalent to Love's

equation for seismic disturbances. Thus Love's equation arises in both extremes of the internal and external plasma β's.

Figure 6 shows that for large exterior magnetic field and for large plasma β inside the tube both fast and slow surface waves exist. We note that here the slab is warmer than its surroundings. Body waves are also present, corresponding to the harmonics described in Paper II and to those described by generalising Equations (22) and (23). From the figure it may be seen that for this situation the Alfvén velocity inside the slab is not itself significant, except insofar as it determines the 'tube' speed c_T inside the slab. The slow surface waves are confined to a region between the 'tube' speeds in the interior and exterior regions. The transverse kink mode, which has phase-speed approximately equal to v_{Ae} for a slender slab, is here a fast surface wave described by Equation (18a), in contrast to the v_{Ae} mode of Figure 3, where, for small exterior field, Equation (19) gives the behaviour.

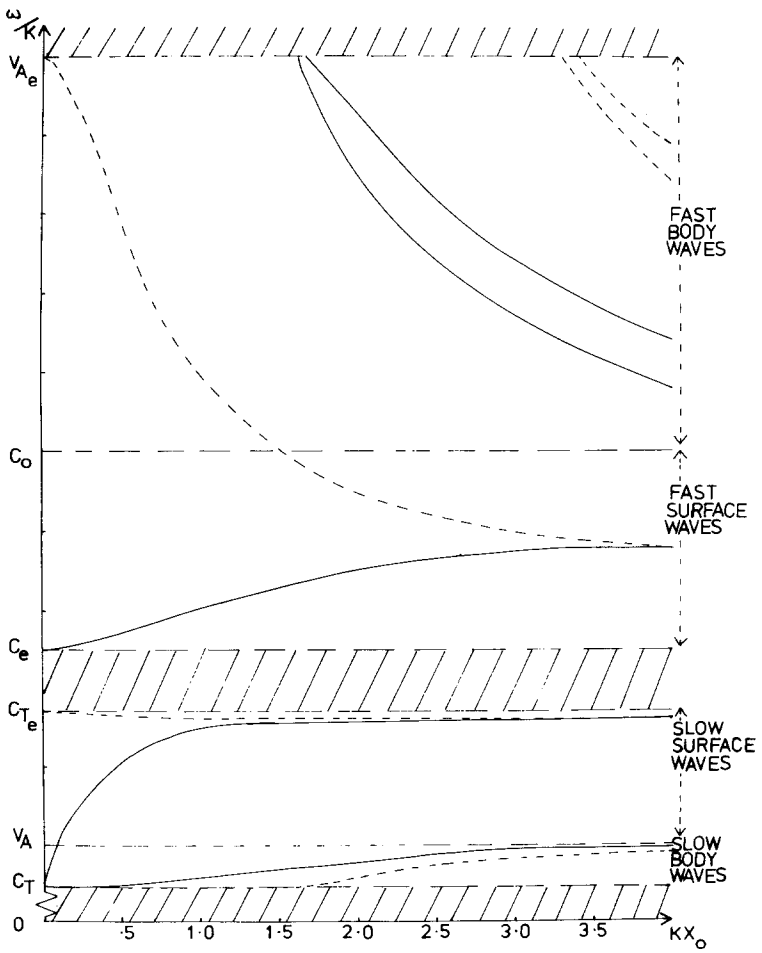

Fig. 6. The phase-speed ω/k as a function of kx_0, showing both fast and surface ($m_0^2 > 0$) and body ($m_0^2 < 0$) waves; here $v_{Ae} = 1.5c_0$, $c_e = 0.75c_0$ and $v_A = 0.5c_0$. Only two typical body waves of the infinite number occurring in $c_T < \omega/k < v_A$ are illustrated. The hatching denotes regions in which modes do not occur. ———: Sausage mode; – – – –: Kink mode.

Notice that for $\omega/k < c_{Te}$ Figures 5 and 6 illustrate the same behaviour. Only the relative values of the sound and Alfvén speeds in the exterior have been interchanged. As a result, the fast surface waves are present in the large external magnetic field situation described in Figure 6 but not in that described in Figure 5.

Finally, Figure 7 illustrates a large exterior field situation in which three bands of body waves occur. Besides the familiar slow body waves confined to the region between c_0 and c_T, we have two bands of fast waves. For a slender slab, presumably because the exterior magnetic field is the dominant feature, these fast waves are

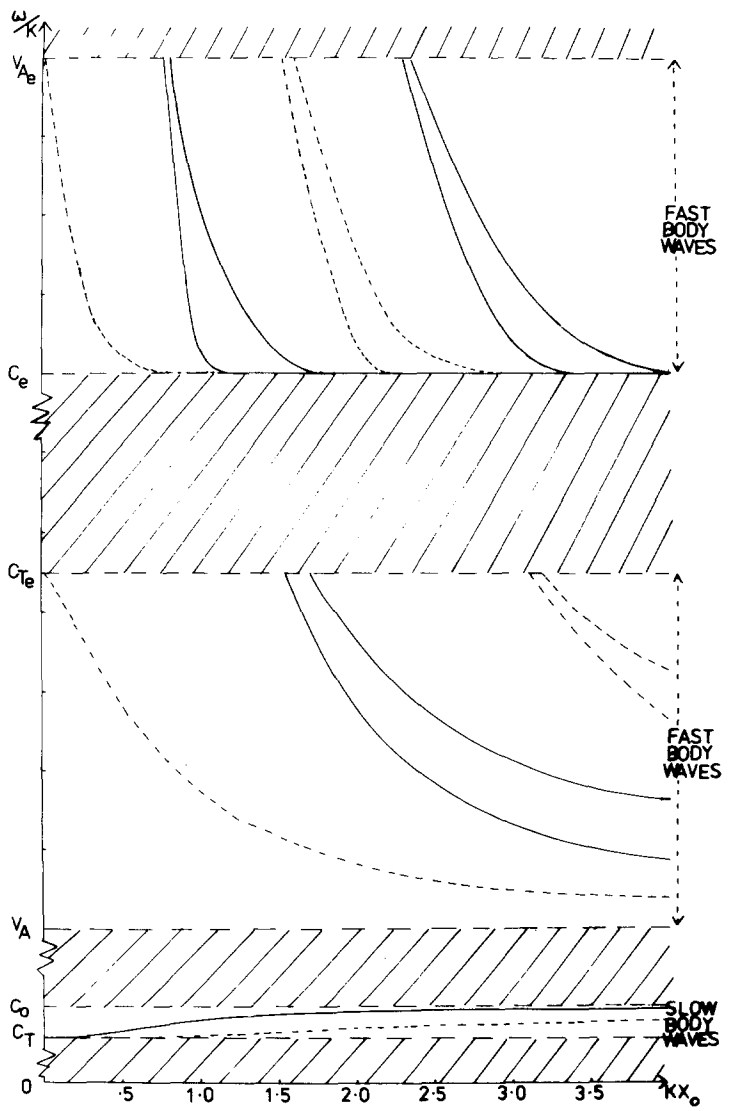

Fig. 7. The phase-speed ω/k as a function of kx_0, showing three bands of body ($m_0^2 < 0$) waves; here $v_{Ae} = 5.0c_0$, $c_e = 4.0c_0$ and $v_A = 2.0c_0$. The narrow band of slow waves contains infinitely many modes of which only two are shown. Hatching denotes regions in which modes do not occur. ———: Sausage mode; – – – –: Kink mode.

TABLE I

The four types of wave, fast or slow, body or surface, which may be present in the four configurations, (i) to (iv), as a result of variations in the relative magnitudes of the sound and Alfvén speeds, are displayed.

√ (followed by a qualifying statement): Indicates the type of mode that occurs (described on the left of the row) for the configuration given at the head of the column. The figures referred to give a general illustration of the wave.

– Indicates that no waves are possible.

The body/surface waves are further subdivided into their typical phase-speeds in a slender slab. $v_\perp$ and $v_\parallel$, respectively, indicate that the motion is principally transverse to, or along, the magnetic field direction.

(For example, for a photospheric situation in which $v_{Ae} \ll c_0$, v_A, c_e and $c_0 > v_A$, say, column (i) shows that 7 of the classified modes are possible, two of which (the slow surface c_{Te} and fast body c_{Te}) are immediately discounted because of the restriction on v_{Ae}.

The waves present in a typical coronal situation v_A, $v_{Ae} \gg c_e$, c_0 are easily deduced from column (iv), which lists the two sets of body waves illustrated in Figure 4 and further emphasises the fact that only the slow waves exist if the Alfvén speeds are interchanged.)

Type of wave		Slender slab	(i) $v_{Ae} < c_e$ $v_A < c_0$	(ii) $v_{Ae} < c_e$ $v_A > c_0$	(iii) $v_{Ae} > c_e$ $v_A < c_0$	(iv) $v_{Ae} > c_e$ $v_A > c_0$
Body waves	slow $< \min(c_0, v_A)$	c_T sausage $v_\parallel$	√ except when $\max(v_{Ae}, c_e) < c_T$ Figures 3, 5			Figures 4, 6, 7
	fast $> \max(c_0, v_A)$	v_{Ae} kink $v_\perp$	–	–	√ for $\max(v_A, c_0) < v_{Ae}$ Figures 4, 6, 7	
		c_e sausage $v_\parallel$	√ for $\max(v_A, c_0) < c_e$ Figure 5		–	–
		c_{Te} kink $v_\perp$		only for $c_{Te} > \max(v_A, c_0)$ Figure 7		

Surface waves	slow < min (c_0, v_A)	v_{A_e} kink $v_\perp$	√ for $v_{A_e} < c_T$ Figure 3		–	–
		c_{T_e} kink $v_\perp$	√ $c_0 > c_e > v_{A_e} > v_A$ (or c_0 and c_e interchanged Figure 5	–	√ $v_{A_e} > c_0 > c_e > v_A$ (or c_0 and c_e interchanged) Figure 6	–
		c_T sausage $v_\parallel$	√ for min (v_{A_e}, c_e) < c_T < max (v_{A_e}, c_e) Figure 3		–	–
	fast > max (c_0, v_A)	v_{A_e} kink $v_\perp$	–	√ for $c_e > v_A > v_{A_e} > c_0$ and $v_A > c_e > v_{A_e} > c_0$	√ for $c_0 > v_{A_e} > c_e > v_A$ Figure 6 and $c_0 > v_{A_e} > v_A > c_e$ (or v_A and v_{A_e} interchanged)	–
		c_e sausage $v_\parallel$	$c_0 > v_A > c_e > v_{A_e}$	$v_A > c_e > v_{A_e} > c_0$ $v_A > c_e > c_0 > v_{A_e}$ Figure 3 (or c_e and c_0 interchanged)	$c_0 > v_{A_e} > c_e > v_A$ $c_0 > v_A > v_{A_e} > c_e$ $v_{A_e} > c_0 > c_e > v_A$ Figure 6	–

the transverse modes, v_{Ae} and c_{Te}, being given by Equations (18a) and (18b) respectively. It may be noted that the fast waves of Figure 6 would exhibit a similar two-band feature were the slab cooler than its surroundings.

Figures 1 to 7 obviously do not exhaust all possibilities for the relative magnitudes of c_e, v_{Ae}, c_0, and v_A, so in Table I we summarise the possible modes which could occur in a given solar context. It must be remembered that these results apply only to waves which are evanescent in the exterior of the slab.

4. Concluding Remarks

The possible normal modes of vibration of a uniform magnetic slab of field embedded in a uniform magnetic atmosphere are many and varied. As a result of categorising them into slow and fast, body and surface, waves it is seen that for certain configurations, for example $v_{Ae} > c_0 > c_e > v_A$, it is possible for all four classes of waves to be present. For propagation along such a field, provided the width of the magnetic slab is very much less than the longitudinal wavelength, the kink mode oscillates transversely with a slow phase-speed close to c_{Te} and a fast phase-speed close to the Alfvén speed v_{Ae} in the surrounding medium. The sausage mode, as described by Roberts (1981b), vibrates with a slow phase-speed near c_T. The faster mode, with phase-speed close to the sound speed c_e in the surrounding atmosphere, is also present but for a non-zero magnetic exterior the limitation, expressed in Paper II, that the slab be cooler than its environment is no longer necessary.

Under circumstances representative of the corona (e.g. $v_{Ae} > v_A > c_0 > c_e$), however, only the slow and fast body waves are present for this two-dimensional situation. The modes of vibration of a slender slab of field under these coronal conditions are a pulsation propagating with phase-speed close to c_T and a transverse motion moving with phase-speed near to that of the exterior's Alfvén speed.

A numerical investigation of the transcendental equation governing the body waves describes their general form but various simplifications, such as the cold-plasma approximation, show that these waves are mathematically analogous to the Love waves of seismology, which propagate as a result of multiple reflections along a layer of the Earth's surface.

The importance of the 'tube' speed c_T is again apparent. For small (or zero) magnetic field external to the slab, c_T forms the upper bound to the slow magnetoacoustic wave, but once the magnitude of the exterior field is sufficiently increased, waves can no longer propagate at phase-speeds below c_T and it becomes the lower bound for propagation.

In summary, then, wave propagation in a magnetically structured atmosphere (such as the slab in a magnetic environment, as discussed here) exhibits a complex array of modes, involving both body and surface waves. No simple description of the allowable modes seems possible, each case requiring investigation in its own right. We have presented here a guide to some of the allowable wave structures,

exhibiting wave diagrams for a number of cases of solar interest including both photospheric and coronal extremes. Detection and identification of such magnetoacoustic waves will be far from easy (but see Giovanelli (1975) for a possible identification, and comments by Wentzel (1979b)), but we await with interest developments in this area.

Acknowledgement

P. M. Edwin acknowledges financial support from the Open University.

Appendix: Dispersion Relations for a Slender Slab

The dispersion relations (15) and (17) for the sausage and kink modes in a slender slab of field, valid for longitudinal wavelengths much greater than the width of the slab, and weak transverse variations, may be derived by using the slender flux tube equations *ab initio*.

Consider first the *sausage* mode. Longitudinal disturbances in a slender slab of field are governed by (see Paper II, Section 3)

$$\frac{\partial^2 v_z}{\partial t^2} - c_T^2 \frac{\partial^2 v_z}{\partial z^2} = -\frac{1}{\rho_0}\left(\frac{c_T}{v_A}\right)^2 \frac{\partial^2 \delta p_{Te}^{(bdy)}}{\partial z\, \partial t}. \tag{A1}$$

Here $\delta p_{Te}^{(bdy)}$ refers to the *total* (gas plus magnetic) pressure perturbation evaluated on the boundary of the slab.

Denoting the velocity in $|x| > x_0$ by $\mathbf{v}_e$ and the external gas pressure variation by δp_e, Equation (A1) may be written

$$\frac{\partial^2 v_z}{\partial t^2} - c_T^2 \frac{\partial^2 v_z}{\partial z^2} = -\frac{1}{\rho_0}\left(\frac{c_T}{v_A}\right)^2 \left\{\frac{\partial^2 \delta p_e}{\partial z\, \partial t} + \frac{B_e^2}{\mu}\frac{\partial}{\partial z}\left(-\frac{\partial v_{e_x}}{\partial x}\right)\right\}^{(bdy)}, \tag{A2}$$

where we have used the z-component of the induction equation to eliminate the external magnetic field variation.

If we also consider the x-component of the momentum equation in the exterior medium $|x| > x_0$, differentiate with respect to t and use the x- and z-components of the induction equation, then we obtain

$$\rho_e \frac{\partial^2 v_{e_x}}{\partial t^2} = -\frac{\partial^2}{\partial x\, \partial t}(\delta p_e) + v_{Ae}^2 \rho_e \left\{\frac{\partial^2 v_{e_x}}{\partial x^2} + \frac{\partial^2 v_{e_x}}{\partial z^2}\right\}. \tag{A3}$$

We now Fourier analyse using the expressions

$$v_z = \hat{v}_z\, e^{i(\omega t + kz)}, \qquad v_{e_x} = \hat{v}_{e_x}(x)\, e^{i(\omega t + kz)}, \qquad \delta p_e = P_e(x)\, e^{i(\omega t + kz)},$$

where P_e and $\hat{v}_{e_x}$ have the form $e^{-m_e(x - x_0)}$ for $x > x_0$ (see Equations (2) and (10) of the main text). In addition, we require that the normal component of velocity be continuous across the boundary and, for a slender tube, that v_x vary from 0 at $x = 0$

to $v_x(x_0)$ at $x = x_0$ in an approximately linear fashion,

$$v_x(x_0) \simeq x_0 \left.\frac{\mathrm{d}v_x}{\mathrm{d}x}\right|_{x=0}. \tag{A4}$$

Utilising Equation (4) of the main text, we may thus write

$$v_{e_x}|_{x=x_0} = v_x|_{x=x_0} \simeq \frac{\hat{v}_z(k^2c_0^2 - \omega^2)x_0}{ikc_0^2}. \tag{A5}$$

Thus, Equation (A2) becomes

$$(k^2c_T^2 - \omega^2)\hat{v}_z = -\frac{c_T^2}{\rho_0 v_A^2}\left\{-P_e(x_0)\omega k + v_{Ae}^2\rho_e m_e \frac{\hat{v}_z(k^2c_0^2 - \omega^2)x_0}{c_0^2}\right\}. \tag{A6}$$

Finally, applying Equation (A3) at the slab boundary $x = x_0$, in conjunction with Equation (A5), and eliminating $\hat{v}_z$ and $P_e(x_0)$ between the resulting equation and (A6), gives the dispersion relation (15) of the main text. Thus we have recovered the equation governing the sausage mode by a much simpler argument than that needed in deriving (15), but at the expense of considering only a slender slab.

The dispersion relation for the *kink* mode follows by applying the argument of Parker (1979) to a slender slab. If we consider the transverse motions of an element of slab width $2x_0$ and unit lengths in the y- and z-directions, the equation of motion for small disturbances ξ in the x-direction is

$$\rho_0 2x_0 \frac{\partial^2\xi}{\partial t^2} = 2x_0 \frac{\mathscr{T}}{R_c} - [\delta p_e(x_0) - \delta p_e(-x_0)], \tag{A7}$$

where $\mathscr{T}$ is the tension in the magnetic field and R_c is the radius of curvature ($=\partial^2\xi/\partial z^2$ to linear order). Here we have assumed that for small disturbances, $|\xi| \ll x_0$, the pressure at the disturbed boundary, $p_e(\xi + x_0)$, equals $\delta p_e(x_0)$ to linear order, with a similar assumption for the boundary $x = -x_0$.

Now, using Equations (4) and (10) of the main text, we may express (A7) in the form

$$\rho_0 2x_0 \frac{\partial^2\xi}{\partial t^2} = 2x_0\rho_0 v_A^2 \frac{\partial^2\xi}{\partial z^2} - \{\delta p_e(x_0) - \delta p_e(-x_0)\}, \tag{A8}$$

where

$$\delta p_e(x_0) - \delta p_e(-x_0) = \frac{-i\rho_e}{\omega}\frac{\{k^2c_e^2v_{Ae}^2 - \omega^2(c_e^2 + v_{Ae}^2)\}}{(k^2c_e^2 - \omega^2)} m_e(\alpha_e + \beta_e).$$

Since $v_x = \partial\xi/\partial t$, for $\xi = \hat{\xi}(x)\, e^{i(\omega t + kz)}$ we have $v_x = i\omega\xi$. Now if both sides of the slab are displaced by equal amounts ξ_0, say, continuity of the normal component of velocity across its boundaries means

$$\alpha_e + \beta_e = 2i\omega\xi_0. \tag{A9}$$

If we now use (A9) together with the information in (A8) we recover dispersion relation (17) of the main text for the kink mode of oscillation in a slender slab.

References

Chakraborty, B. B.: 1968, *Prog. Theor. Phys.* **40**, 210.
Defouw, R. J.: 1976, *Astrophys. J.* **209**, 266.
Ewing, W. M., Jardetzky, W. S., and Press, F.: 1957, *Elastic Waves in Layered Media*, McGraw-Hill.
Giovanelli, R. G.: 1975, *Solar Phys.* **44**, 299.
Goedbloed, J. P.: 1971, *Physica* **53**, 412.
Love, A. E. H.: 1911, *Some Problems of Geodynamics*, Chapter XI, C.U.P.
Parker, E. N.: 1979, *Cosmical Magnetic Fields*, Chapter 8, Oxford.
Roberts, B.: 1981a, *Solar Phys.* **69**, 27 (Paper I).
Roberts, B.: 1981b, *Solar Phys.* **69**, 39 (Paper II).
Roberts, B. and Webb, A. R.: 1978, *Solar Phys.* **56**, 5.
Roberts, B. and Webb, A. R.: 1979, *Solar Phys.* **64**, 77.
Spruit, H. C.: 1982, *Solar Phys.* **75**, 3.
Uberoi, C. and Somasundaram, K.: 1980, *Plasma Phys.* **22**, 747.
Webb, A. R.: 1980, Ph.D. Thesis, St. Andrews University.
Wentzel, D. G.: 1979a, *Astrophys. J.* **227**, 319.
Wentzel, D. G.: 1979b, *Astron. Astrophys.* **76**, 20.
Wilson, P. R.: 1980, *Astron. Astrophys.* **87**, 121.